

## Characterizing Tourmaline in Metapelitic Schists from The Gasht Area, North Iran and Boron Source in Metamorphic Fluids

M. Moazzen<sup>\*1,2</sup>, R. Michaeli<sup>1</sup>, M. Ahangari<sup>3</sup>, and U. Altenberger<sup>4</sup>

<sup>1</sup>Department of Earth Sciences, Faculty of Sciences, University of Tabriz, 51664, Tabriz, Islamic Republic of Iran

<sup>2</sup>Research Institute for Fundamental Sciences (RIFS), 51664, Tabriz, Islamic Republic of Iran

<sup>3</sup>Department of Geology, Faculty of Sciences, University of Urmia, Urmia, Islamic Republic of Iran

<sup>4</sup>Institut für Erd und Umweltwissenschaften, Universität Potsdam, 14476 Potsdam, Germany

Received: 13 April 2016 / Revised: 16 August 2016 / Accepted: 22 October 2016

### Abstract

Metapelitic rocks in the Gasht area include micaschist, kyanite schist, andalusite schist, garnet schist, staurolite schist, cordierite schist and sillimanite schist. Tourmaline occurs as accessory mineral in all of these rock types. These schists are metamorphosed regionally and are affected by contact metamorphism subsequently. Based on the textural relations and the fact that CaO and TiO<sub>2</sub> contents in the studied tourmalines are low, they are formed during regional metamorphism. They appear in the rock matrix and as inclusions in other minerals, especially biotite and albite. The studied tourmalines are of alkali type and are rich in dravite end-member. Cl and F contents are below the detection limit testifying for hydro-tourmaline nature of the studied minerals. Na and K are higher in the X-site in comparison with Ca. Low Ca shows negligible amounts of Ca end-member or uvite. Mg content is much higher than Fe in the structure of the studied tourmalines, which are not zoned or show weak zoning and are grown at nearly constant P-T conditions. These tourmalines are crystallized from pelitic to psammitic protoliths in equilibrium with a fluid phase, rich in Al. Boron in fluid more likely was from the boron adsorbed on clay minerals surface in the protolith, released during metamorphism and boron from B-bearing mica breakdown during high temperature metamorphism, while boron released from the subducting oceanic crust is not a likely source for tourmaline crystallization in the studied rocks since there is no evidence for tourmaline in the associated oceanic crust mafic rocks.

**Keywords:** Tourmaline; Dravite, Metapelites, Metamorphic Fluids.

### Introduction

Tourmaline is an accessory mineral in many rock

types, which can be found in different geological settings [5, 10]. The vast chemical composition of tourmaline is a reflection of the environment in which it

\* Corresponding author: Tel: +984133393922; Fax: +984133250399; Email: moazzen@tabrizu.ac.ir

crystallizes. Tourmaline occurs in a variety of lithologies and is stable over an exceptionally large P–T range, including conditions in subducting slabs up to a depth of ~250km [3, 22, 41]. Growth and stability of this widespread borosilicate in subducting metasediments is thought to be responsible for recycling of B with an isotopic composition influenced by surface processes into the deep mantle. The stability of tourmaline is controlled by factors such as B and Al activity, temperature, H<sub>2</sub>O activity and the amount of elements such as P, Mg and Fe. B and Al are more important in this regard [3]. The chemical variety of tourmaline results in 11 different types of this mineral among which schorl, dravite and elbaite are the most important [2, 16, 37]. Hawthorne and Henry [12] consider the formula  $XY_3Z_6(T_6O_{18})(BO_3)_3V_3W$  for tourmaline in which the X crystallographical site includes X-vacancy, K, Na and Ca [4]. The Y crystallographical site includes Li, Mg, Fe<sup>2+</sup>, Mn, Al, Cr<sup>3+</sup>, V<sup>3+</sup>, Fe<sup>3+</sup> [37]. This site tolerates diverse substitutions involving monovalent, divalent, trivalent and quadrivalent cations. The Z site accommodates mainly Mg and Al. Fe<sup>3+</sup>, V<sup>3+</sup>, Cr<sup>3+</sup> and Ti<sup>4+</sup> can

replace Al in this site. The T site is filled by Si and Al and V and W are the sites for OH and F. Boron occurs in regular triangular coordination and has no apparent substituents. Element substitution in the Y site forms different types of tourmaline. For instance, Fe<sup>2+</sup> and Mg in this site make schorl and dravite respectively and Li and Al substitution makes elbaite. Substitutions in tourmaline can take place as homovalent cation exchanges on a single site (such as Mg for Fe<sup>2+</sup> in the Y site) or as heterovalent coupled substitutions over several sites (such as the coupled uvite substitution (Ca-Mg for Na-Al) involving the X and Z sites). According to van Hinsberg et al. [38] tourmaline can adjust its composition to suit a wide variety of environments, and therefore displays a remarkable range in stability in terms of pressure, temperature, the host rock and the fluid composition. They estimated the stability field of tourmaline on pressure-temperature diagram (Fig. 1). This mineral can be found in many detrital sedimentary rocks along with other heavy minerals, resistant against chemical and mechanical changes. Tourmaline is a suitable mineral in deciphering the metamorphic-hydrothermal events [13]. Therefore it

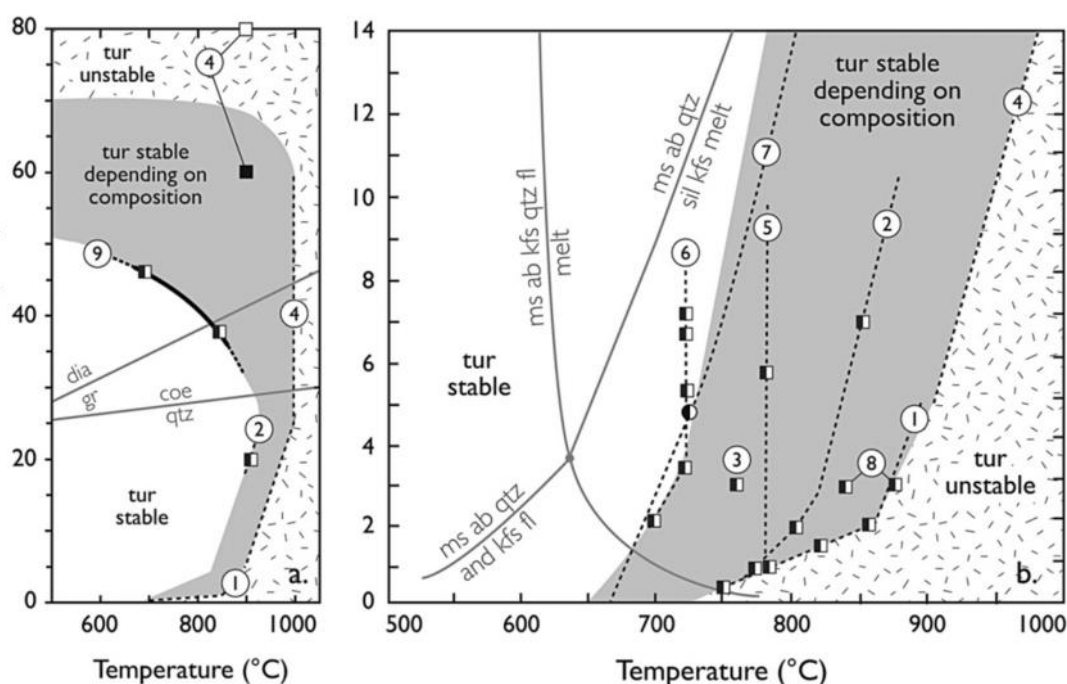


**Figure 1.** P–T stability of tourmaline with different compositions, with high-P stability shown in (a). Circles represent constraints from natural samples, squares are experimental data, and dashed lines, the extrapolations presented by the original authors (From [38]). The curves for H<sub>2</sub>O-saturated melting reactions, and the quartz–coesite and graphite–diamond phase transitions are shown for reference. Data are for: 1) dravite: [33], 2) magnesio-foitite: [40], 3) schorl: [18], 4) dravite: [21], 5) Na-free Mg system: [39], 6) Na-bearing Mg system: [39], 7) natural tourmalines: [19], 8) natural tourmaline: [34], 9) dravite: [31]. Mineral name abbreviations are from [20].

provides substantial information on development of both sedimentary and metamorphic rocks and is an important indicator of provenance in clastic sedimentary and metasedimentary rocks. Tourmaline is existent in metamorphic rocks in a wide range of protoliths, whole rock compositions and metamorphic grades [3, 14]. It can be stable with other mineral phases at temperatures close to the earth surface temperature, up to the temperatures at the granulite facies metamorphism and

at pressures from the surface pressure up to 60 kbars [8]. Tourmaline typically exhibits chemical zoning at low grade metamorphic rocks, pointing to mineral reactions occurred during progressive metamorphism [14].

Tourmaline occurs as accessory mineral in the pelitic schists from the Gasht area in north Iran. Although it is an accessory mineral, but it has considerable modal percentage in many samples studied (up to 5 modal%).

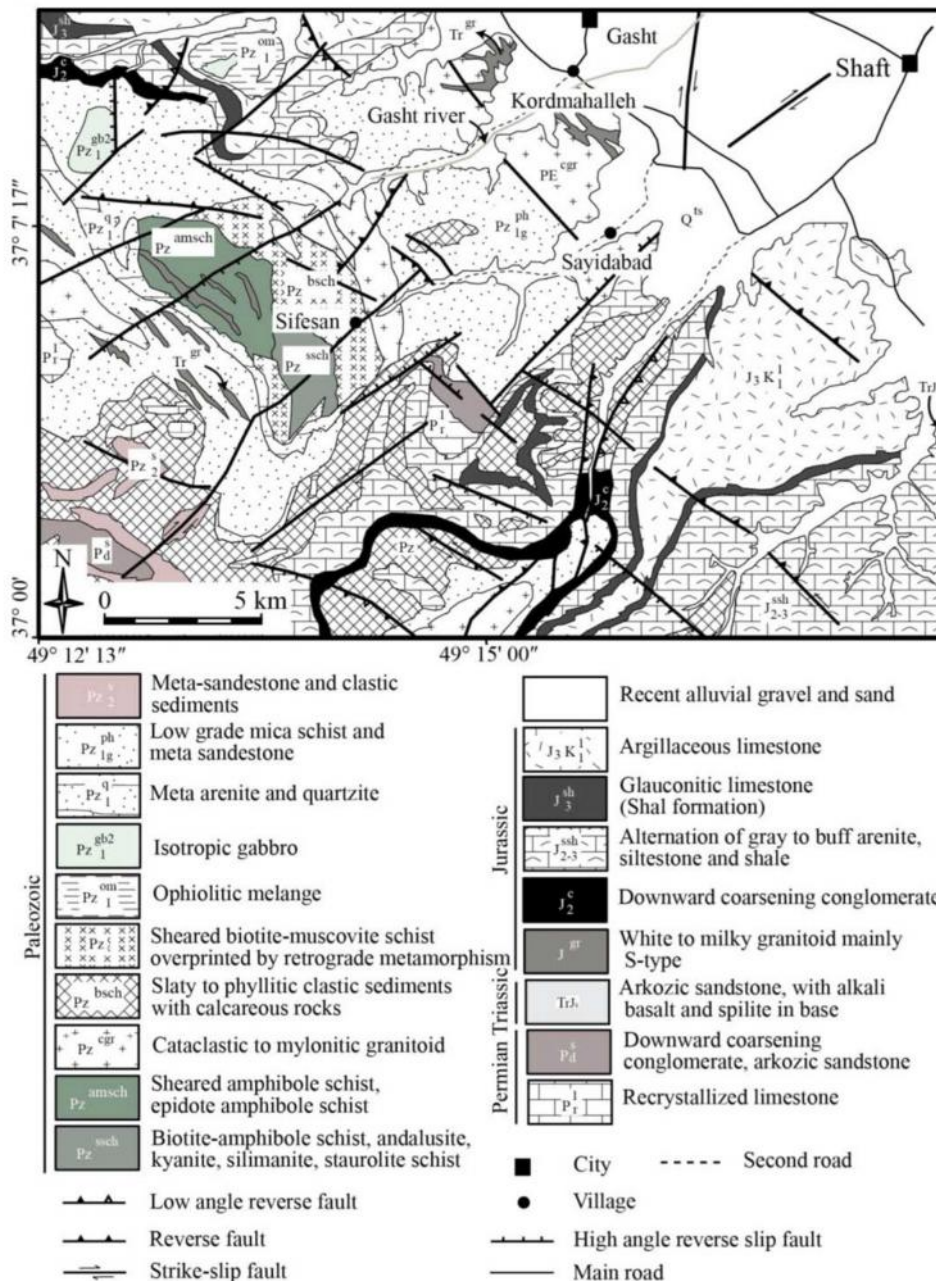


Figure 2. Geological map of the Gasht area

We have used the chemistry of tourmaline in these rocks in order to identify the tourmaline type, its chemical features and its bearing on characterizing metamorphic fluids.

### The Geological Background

The Gasht metamorphic complex is located at the south of Fuman town and the east of Masuleh village in northern Iran. Various metamorphic and igneous rocks are exposed in this area (Fig. 2). Davis et al. [7] consider the Gasht metamorphic complex as two distinct sequences formed from volcanic and sedimentary rocks, which are separated by a hypothetical unconformity. According to these researchers, the lower sequence is made of gneiss and schists with aluminosilicates, biotite, quartz and albite, while the

upper sequence is made of slate, schist and quartzite with metaconglomerate interlayers. Using Rb/Sr dating method, Crawford [6] estimated ages of  $382\pm 14$  and  $375\pm 12$  Ma for the porphyroblastic gneiss and schists of the area, respectively. These ages indicate a metamorphic event at late Devonian. The rock units in the area are old metamorphic rocks of the Talesh mountain and metamorphic rocks of the Asalam-Shanderman complex [29] including schist, phyllite, metapsammite and quartzites, mafic lavas, and fossil-bearing lower Palaeozoic limestones. The Carboniferous units are limestone associated with andesitic volcanic rocks and cherts. The Shemshak formation, Lar limestone and Shal glauconite-bearing sandstones with a Jurassic age are covered by Cretaceous andesite and andesite-basalt (Fig. 2). Different types of intrusive

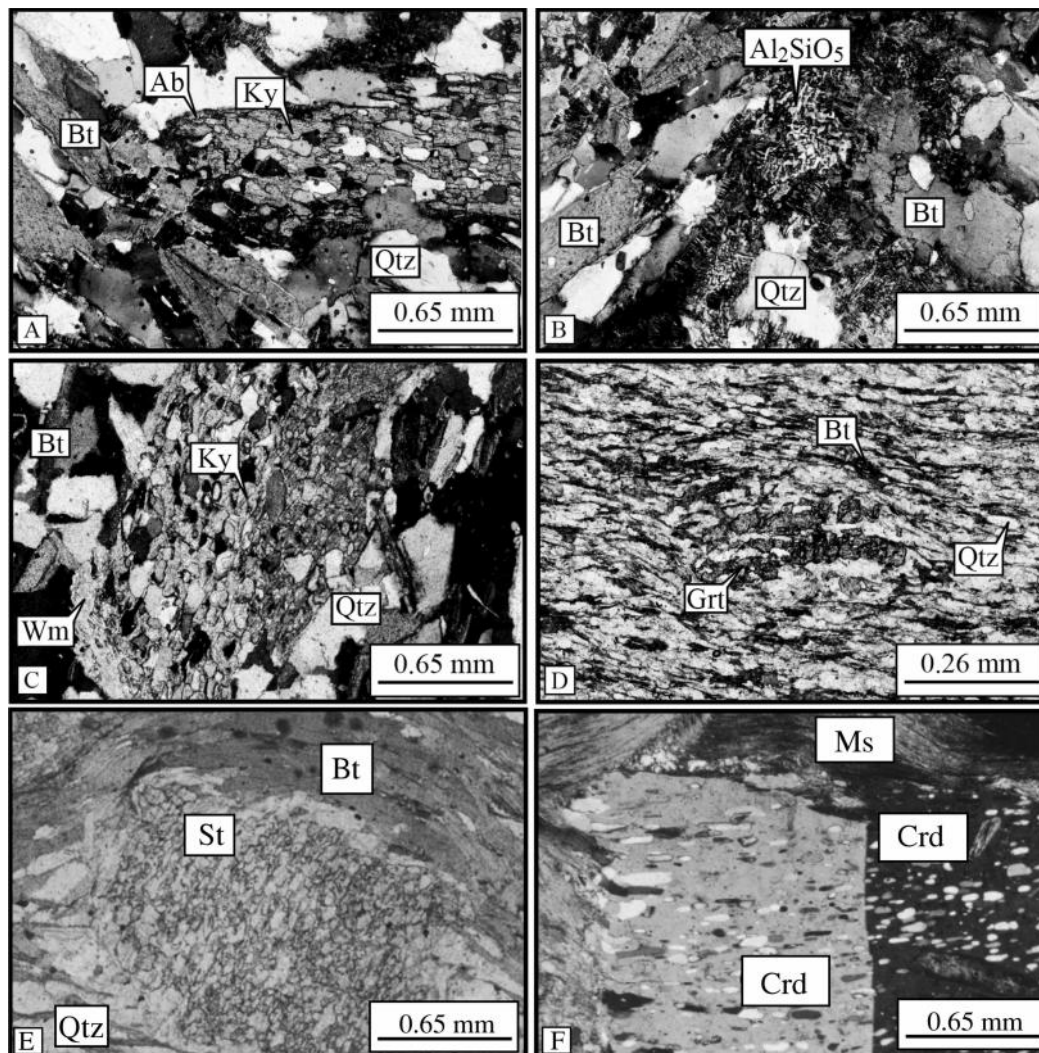


**Figure 3.** Mineralogical composition and textural relations in the Gasht metapelites. A) kyanite schist, B) andalusite schist, C) kyanite -white mica schist, D) garnet-mica schist, E) staurolite schist and F) cordierite schist. Mineral name abbreviations are from [20].

igneous rocks including gabbro, diorite and granite [30] intruded the Gasht slates, phyllites and schists. Tourmaline crystals studied in this contribution are from the Gasht schists.

#### **Petrography Of Tourmaline-Bearing Pelitic Schists**

Metapelitic rocks of the Gasht complex are micaschist, kyanite schist (Fig. 3A and 3C), andalusite schist (Fig. 3B), garnet schist (Fig. 3D), staurolite schist (Fig. 3E), cordierite schist (Fig. 3F) and sillimanite schist. Muscovite and biotite make the main rock foliation and the lepidoblastic texture. Porphyroblastic texture is a result of relatively larger garnet, andalusite and cordierite crystals in a finer groundmass. Garnet is formed as skeletal crystals with plenty of inclusions and poikiloblastic texture (Fig. 3D). Two main deformational phases can be seen in the rocks, D1 and D2. The D2 deformational phase is the main and the pervasive phase in the rocks, which has abolished the D1 deformational features and only traces of S1 is remained. M1 metamorphism is associated with the D1 deformation and the M2 metamorphism with the D2 deformation. Injection of granitoids in the area has imposed a late contact metamorphism on the previously regionally metamorphosed rocks. This late contact metamorphism is picked up by post-deformation crystallization of cordierite in the rocks (Fig. 3F). The accessory minerals in the Gasht pelitic schists are tourmaline, zircon, apatite and opaque minerals. Tourmaline appears in the rock matrix and as inclusions in other minerals, especially biotite (Fig. 4A) and albite (Fig. 4B). It is up to 0.3 mm in size and occasionally shows optical zoning, however is mainly homogeneous. Tourmaline crystals in the Gasht metapelites are arranged within the main foliation and are regional metamorphic, based on the textural relations.

#### **Tourmaline Mineral Chemistry**

Representative samples, well-defined by optical microscopy, were chosen for mineral chemistry. A JEOLJXA-8900K superprobe in Institute for Earth and Environmental Sciences, University of Potsdam, Germany was used for microprobe analysis and obtaining electron back scattered images. Analyses were performed at 15 kV and 20 nA specimen current with a 2–10  $\mu\text{m}$  diameter beam. Counting time was 10–30 seconds on peaks and half-peak on background. Natural and synthetic standards (Fe<sub>2</sub>O<sub>3</sub>[Fe], rhodonite [Mn], rutile [Ti], MgO [Mg], wollastonite [Si, Ca], fluorite [F], orthoclase [Al, K] and albite [Na]) were used for calibration.

The chemical composition of Gasht tourmalines are presented in Table 1. The structural formula of tourmaline is calculated based on 24.5 oxygen atoms. Since the Al content is higher than 6 apfu (atom per formula unit) (6.1 to 6.6), the studied tourmalines are Al-tourmaline [25]. The analytical data show that Cl and F contents are below the detection limit. Therefore the studied tourmalines are hydro-tourmaline. Hawthorne and Henry [12] classified tourmalines based on K, Na, Ca and the X-vacancy in three groups of alkali and calcic tourmalines and tourmalines with X-vacancy site. Gasht tourmalines plotted on the triangular diagram of Hawthorne and Henry [12], are alkali tourmalines in this scheme (Fig. 5). This shows higher Na and K in the X-site in comparison with Ca. Low Ca shows negligible amounts of Ca end-member or uvite (Ca(Fe, Mg)(Na, Al)-1) in the studied tourmalines.

In order to distinguish the tourmaline type in the Gasht metapelites, diagrams of Trumbull and Chaussidon [36] and Hawthorne and Henry [12] are used. Based on these diagrams (Fig. 6) the tourmalines are dravite. Mg is much higher than Fe in the structure of the studied tourmalines. Diagram of Al<sub>50</sub>Mg<sub>50</sub>-Al<sub>150</sub>Fe<sub>50</sub> [17] can be used to decipher the nature of

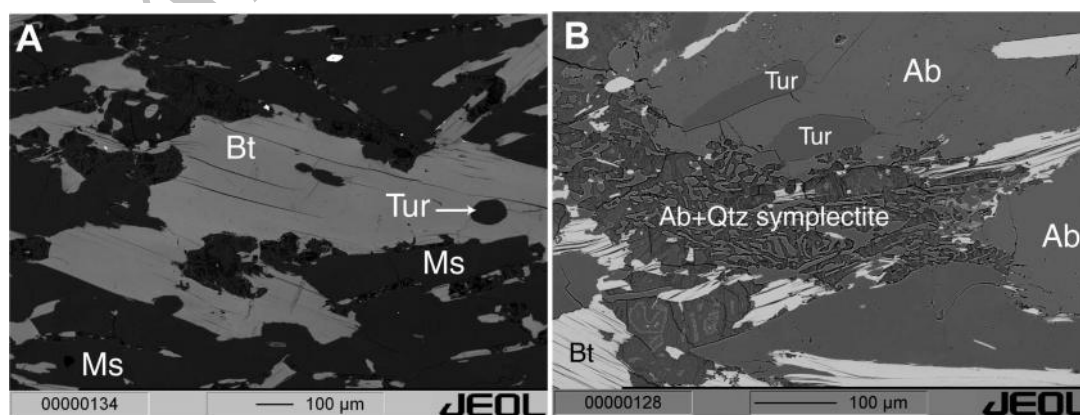


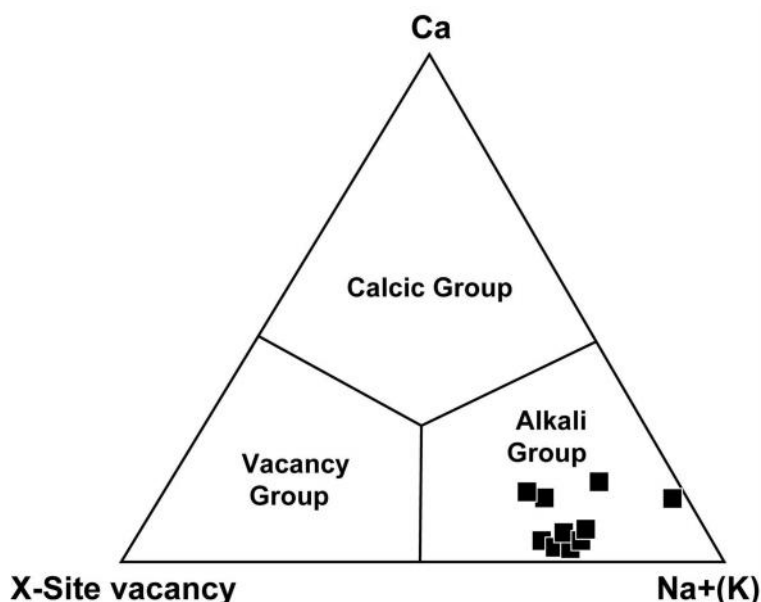
**Figure 4.** Electron back scattered images of tourmaline in biotite (A) and albite (B).

**Table 1.** Microprobe analyses of tourmaline in the pelitic schists of the Gasht metamorphic complex. The structural formula is calculated based on 24.5 oxygen atoms.

Sample	28.1	28.2	27.3	29.1	27.4	26	28.3	29.4	29.3	29.5
SiO <sub>2</sub>	36.32	36.35	35.56	35.86	36.48	36.40	36.29	36.21	35.92	39.96
TiO <sub>2</sub>	0.63	0.36	0.79	0.61	0.63	0.30	0.44	0.73	0.78	0.68
Al <sub>2</sub> O <sub>3</sub>	32.45	32.56	34.26	32.09	32.38	33.27	32.90	33.44	34.24	33.20
Cr <sub>2</sub> O <sub>3</sub>	0.03	0.00	0.06	0.03	0.07	0.02	0.03	0.02	0.03	0.06
FeO	8.78	6.94	5.25	6.87	8.55	8.82	8.60	6.68	6.31	6.06
MgO	5.97	5.66	6.29	5.90	5.98	5.73	5.87	6.43	6.22	5.43
CaO	0.25	0.16	0.76	0.22	0.19	0.13	0.16	0.67	0.74	0.92
Na <sub>2</sub> O	2.34	2.17	1.85	2.17	2.31	2.25	2.20	2.01	2.84	2.25
K <sub>2</sub> O	0.02	0.03	0.07	0.04	0.02	0.02	0.03	0.02	0.05	0.14
Total	86.79	84.23	84.92	83.78	86.61	86.96	86.52	86.21	87.13	88.72
Si	5.941	6.044	5.832	6.005	5.968	5.931	5.939	5.894	5.801	6.270
Ti	0.078	0.045	0.097	0.077	0.078	0.037	0.054	0.089	0.095	0.081
Al	6.256	6.381	6.622	6.333	6.243	6.389	6.346	6.415	6.517	6.140
Cr	0.004	0.000	0.007	0.003	0.009	0.003	0.003	0.002	0.004	0.008
Fe <sup>++</sup>	1.201	0.965	0.720	0.962	1.170	1.202	1.177	0.909	0.852	0.795
Mg	1.456	1.403	1.538	1.473	1.458	1.392	1.432	1.560	1.497	1.270
Ca	0.044	0.029	0.134	0.039	0.033	0.022	0.028	0.117	0.128	0.155
Na	0.742	0.700	0.588	0.705	0.733	0.711	0.698	0.633	0.889	0.684
K	0.004	0.006	0.014	0.007	0.004	0.004	0.005	0.005	0.011	0.028
Total	15.725	15.573	15.557	15.606	15.697	15.694	15.684	15.627	15.794	15.431

fluids involved in tourmaline crystallization. Based on this diagram (Fig. 7), Gasht tourmalines plot in the metapelite and metapsammite field, originated from Al-rich fluids. Regional and contact metamorphic tourmalines can be distinguished by their Ca content. Ca in regional metamorphic tourmalines is very low (<0.4),

while it is higher in contact metamorphic tourmalines (0.4-1.9). Usually K<sub>2</sub>O, Cr<sub>2</sub>O<sub>3</sub> and MnO concentration is lower than 0.5 in this type of tourmalines. TiO<sub>2</sub> content in contact metamorphic tourmalines reach 1.7 wt %. AlIV in regional metamorphic tourmalines is <0.1 and it reaches 0.1 to 0.35 apfu in contact metamorphic

**Figure 5.** Gasht tourmalines classification on the diagram of [12]. All tourmalines belong to the alkali group.

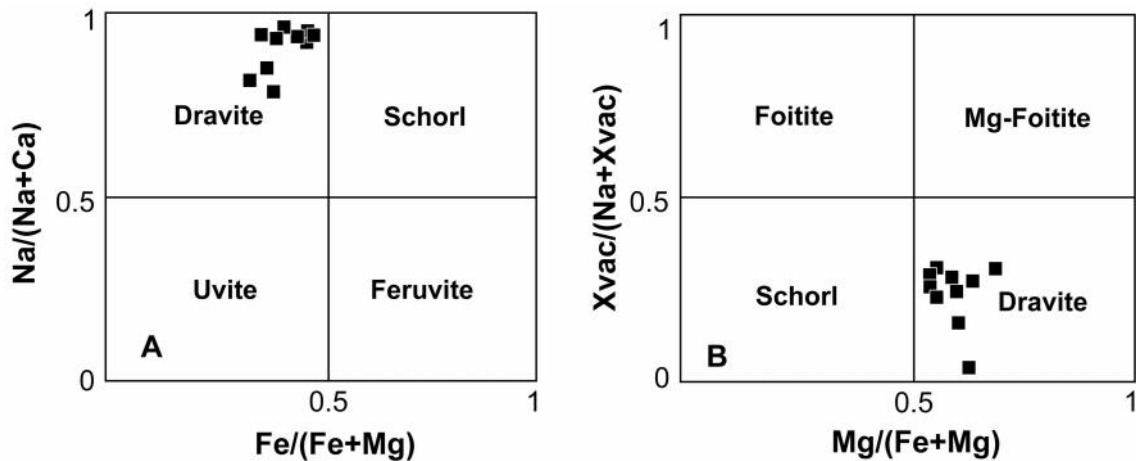


**Figure 6.** Mg/(Fe+Mg) versus Na/(Na+Ca) diagram (A, [35]) and Mg/(Fe+Mg) versus X-vacancy diagram (B, from [12]) for the Gasht tourmalines. All analyzed tourmalines are dravite.

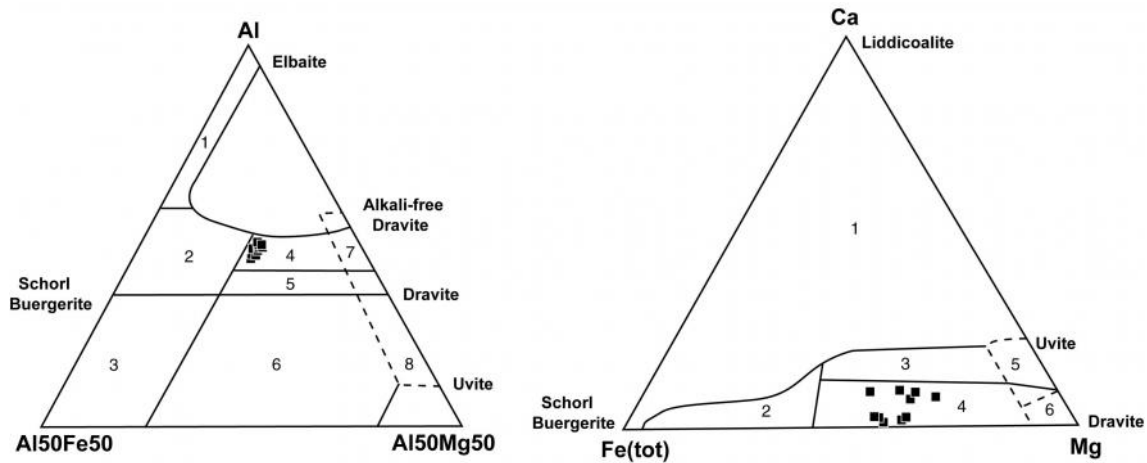


**Figure 7.** Chemistry of tourmaline in different rock types. 1) granitoids, pegmatites and aplites rich in Li, 2) granitoids poor in Li and the related pegmatites and aplites, 3) Fe-rich quartz-tourmaline rocks, 4) metapelites and metapsammities in equilibrium with a Al-rich fluid phase, 5) metapelites and metapsammities in equilibrium with Al-poor fluid phase, 6) calc-silicate rocks, 7) meta-ultramafic rocks with low Ca and metasediments rich in V and Cr, 8) metamorphosed carbonatites and pyroxenites (after [17]).

tourmalines [17]. Considering low CaO and TiO<sub>2</sub> contents in the studied tourmalines, they are formed during regional metamorphism. This is in agreement with textural observations.

Element substitution in tourmaline structure occurs as substitution of cations with similar ionic charge in one single crystallographic site and also substitution of cations with different ionic charges in several sites. Crystal chemistry and substitution vectors in tourmaline are controlled by several basic mechanisms of substitution. In schorl and dravite, there is the alkali-deficient substitution (1)  $R^{+} + R_2^{+} \rightarrow R_3^{+} +$  and the

dehydroxylation type of substitution (2)  $(OH)^{-} \rightarrow R_2^{+} + R_3^{+} + O_2^{-}$  [9]. These trends control the high-Al tourmalines trend in the samples studied. Using R<sub>1</sub>+R<sub>2</sub> versus R<sub>3</sub> diagram (Fig. 8A) it can be seen that the Gasht tourmalines plot along the proton deficient and alkali deficient vectors (Fig. 8A), indicating Al substitution. Substitution of Al in the octahedral site of Y causes proton deficiency. The studied tourmalines have a narrow Ca variation (<0.2), while Na variation is considerable (Fig. 8B). This shows AlNa-1Mg-1 substitution vector in these tourmalines. denotes vacancy in this exchange vector. R<sub>2</sub>\* versus Al in R<sub>2</sub>

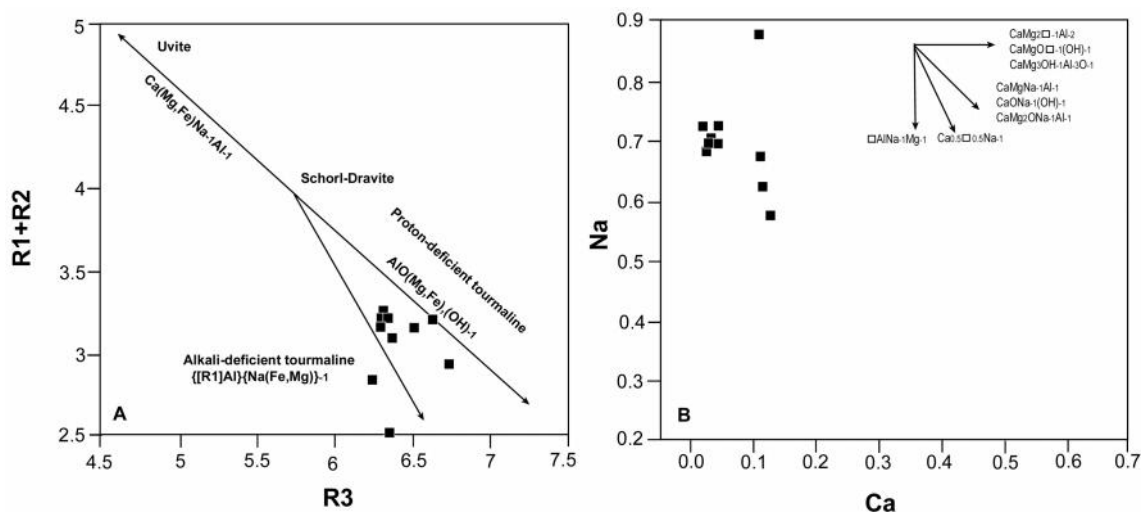


Figure 8. A) Cation substitution in the Gasht tourmalines using  $R_1+R_2$  versus  $R_3$  parameters after [27] ( $R_1=Ca+ Na$ ,  $R_2=Fe+Mg+Mn$ ,  $R_3= Al+1.33Ti$ ). B) Investigation of cation substitution using Na versus Ca diagram.

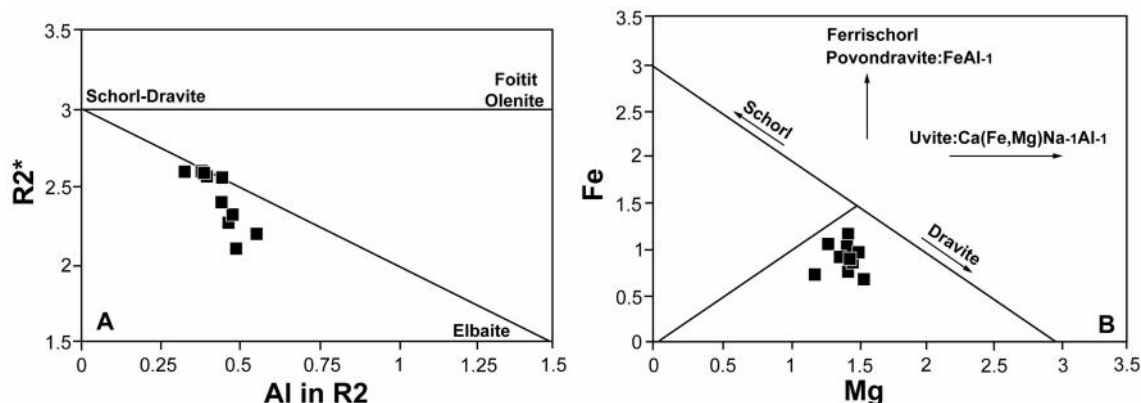


Figure 9. A)  $R_2^*$  versus Al in R2 diagram ( $R_2^*=Fe+Mg+Mn+Al$ ,  $R_2=Al+1.33Ti+Si-12$ ) and B) Fe versus Mg diagram for the Gasht tourmalines. Both diagram show Al in Y substitution for the studied tourmalines.

diagram (Fig. 9A) indicates that the Y octahedral site is not completely occupied by Al. Elbaite substitution (Li exchange) compensates it. This causes Li and Al substitution for Fe and Mg in the Y site (Fig. 9 B, [26]). Fe versus Mg diagram (Fig. 9B), apart from indicating dravite, uvite and Al substitution in the Y site, shows the composition of the tourmalines. Based on this diagram, all studied samples plot blow the schorl-dravite line ( $\Psi:Fe+Mg=3$ ). The lower  $\Psi$  amount shows the higher Al substitution in the Y octahedral site [26]. The high Al substitution in the Y site for the studied tourmalines is due to  $AlOMg-1(OH)-1$  and  $AlNa-1Mg-1$  substitutions (e.g. [11]).

### Results and Discussion

Tourmaline is the first mineral which forms from the aqueous phase following temperature decrease. The main elements for formation of this mineral are B, Al, Fe and Mg after Si. Boron is an incompatible element during crystallization. The Al saturation index (ASI) for tourmaline stability is 3. This mineral becomes unstable in melts in biotite-bearing environment with less than 6 wt%  $B_2O_5$ . The ASI should reach 1.3 to 1.4 to stabilize tourmaline [25].

Clay minerals, especially illite and organic materials are potential source for boron in tourmaline crystallization [14]. Pelites and psammites contain considerable amounts of boron to produce tourmaline by reaction with other minerals in the rock. Tourmaline



is either a sedimentary relict mineral in the pelitic sediments or it crystallizes during prograde metamorphism by B-bearing fluids infiltration. In most cases the source of boron is not known. Tourmaline is found as a mechanical detrital mineral in coarse grained sedimentary rocks. However when the fluids become more alkaline and the activity of ions, especially  $Al^{3+}$ ,  $Mg^{2+}$ ,  $Fe^{3+}$ ,  $Fe^{2+}$ ,  $Na^+$ ,  $B^{3+}$  increases in the fluids, tourmaline becomes unstable and disappears [25]. Four possible sources can be postulated for boron in the protolith: (i) fine tourmaline crystals dissolving and reprecipitating during metamorphism (ii) clay minerals (especially illite) with boron adsorbed to the surface (e.g.[15]). Hot fluids of marine origin can liberate B from clay minerals and become enriched in B [32]. (iii) boron-rich fluids derived from the granitoids in the area [24], (iv) altered oceanic crust that occasionally contains up to 270 ppm B [23] is another possible source for B.

There is no textural evidence in the studied rocks to confirm dissolution and precipitation of tourmaline. Therefore the first mechanism seems not to be responsible for crystallization of tourmaline in the Gasht metapelites. However there is a possibility that former fine-grain tourmalines are dissolved totally and then are precipitated as new crystals leaving no textural evidence behind. This can not be confirmed or ruled out for the studied samples since there is no B stable isotopic data for these rocks. Rise in temperature during prograde metamorphism more likely released boron from the clay minerals in the pelitic protolith. Then boron exerted into the fluid in equilibrium with the metamorphic minerals. The continuation of temperature increase results in dehydration reactions which can lead to boron depletion. This is a reason for lack of tourmaline at high temperatures.

Boron derived from the granitic rocks can not be taken as a source for tourmaline crystallization in the pelitic rocks of the Gasht area since the granites are S-type, originated from partial melting of muscovite-rich metapelites [29]. This means that more likely the source of boron-rich fluids in equilibrium with S-type granitic melt was fluids released from the metapelites. More ever tourmaline in the Gasht schists are regional metamorphic phase based on chemical and textural features. This means that they are crystallized prior to intrusion of the granitoids.

The other possible source for boron in the studied rocks may be boron from the altered oceanic crust (mafic rocks of the Gasht area). Gasht metamorphic rocks are considered to be results of continental collision, following the closure of the Palaeotethys oceanic crust [28]. Since these rocks are subduction-related, boron released from the subducting oceanic

crust can contribute to tourmaline crystallization in these rocks. No tourmaline was observed in the mafic rocks of the Gasht area [28]. Also tourmaline is absent in Shanderman eclogites to the north of the studied area [29]. Therefore boron from the subducting slab as shown by Altherr et al. [1] can not be considered for formation of tourmaline in the Gasht metapelites.

Evidence provided above, testify for boron released from the clay minerals in the pelitic protolith as the main source of B-rich fluids.

Hydrothermal tourmaline crystallizes in the crustal rocks with distinct zoning, while metamorphic tourmaline does not require nucleation on detrital cores. Prograde metamorphic tourmalines lacking detrital cores, typically display discontinuous zoning formed during closed system growth. Alternatively, in an open metamorphic system to fluid infiltration, tourmaline may crystallize during a discrete stage when the system becomes locally enriched by influx of B-bearing fluids. Tourmaline formed in such a condition is generally chemically homogeneous to very weakly zoned. Since tourmaline in the Gasht metapelitic rocks is homogeneous or weakly zoned, more likely it is formed during a discrete stage in an open system for B.

### Acknowledgements

We are grateful to Christina Gunter from the Potsdam University for her help with the microprobe analysis. The field works were supported by University of Tabriz. We thank Dr. A. A. Sepahi and Dr. P. Ba ík for their constructive suggestions on an earlier version of the manuscript.

### References

1. Altherr R., Topuz G., Marschall H., Zack T. and Ludwig T. Evolution of a tourmaline-bearing lawsonite eclogite from Elekdag area (Central Pontides, N Turkey): evidence for infiltration of slab derived B-rich fluids during exhumation. *Contrib. Mineral. Petrol.*, **148**: 409–425 (2004).
2. Ba ík P., Meres S. and Uher P. Vanadium-bearing tourmaline in metacherts from Chvojnica, Slovak Republic: Crystal chemistry and multistage evolution. *Canad. Mineral.*, **49**: 195-206 (2011).
3. Berryman E., Wunder B., Rhede D., Schettler G., Franz G. and Heinrich W. P–T–X controls on Ca and Na distribution between Mg–Al tourmaline and fluid. *Contrib. Mineral. Petrol.*, 171. DOI:10.1007/s00410-016-1246-8 (2016).
4. Berryman E., Wunder B., Ertl A., Koch-Muller M., Rhede D., Scheidl K., Giester G. and Heinrich W. Influence of the X-site composition on tourmaline's crystal structure: investigation of synthetic K-dravite, dravite, oxy-uivite,

- and magnesio-foitite using SREF and Raman spectroscopy. *Physic. Chem. Mineral.*, DOI: 10.1007/s00269-015-0776-3 (2015).
5. Bosi F. and Lucchesi S. Crystal chemical relationships in the tourmaline group: Structural constraints on chemical variability. *Am. Mineral.*, **92**:1054–1063 (2015).
  6. Crawford M.A. A summary of isotopic age data for Iran, Pakistan and India. In: *Libre a la memoire l'a A.F. de l'apparent. Memoire hors-serie 8.Soc. Geolog. de France*, 251-260 (1977).
  7. Davis R.G., Hamzepour G., Jones, C.R. and Clark, G.C. Geology of the Masuleh sheet (Northwest Iran). *Geol. Surv. Iran.*, Report **24**:110 (1972).
  8. Dutrow B., Foster C.T. Jr. and Henry D. J. Tourmaline-rich pseudomorphs in sillimanite zone metapelites: Demarcation of an infiltration front. *Am. Mineral.*, **84**:794–805 (1999).
  9. Dutrow B. and Foster C.T. Jr. Constraints on metamorphic fluid from irreversible thermodynamic modeling of tourmaline pseudomorph formation. *Geol. Soc. Am. Abst. Progr.*, **24**:A218 (1992).
  10. Dutrow B. L. and Henry D. J. Tourmaline: A Geologic DVD. *Elements*, **7**: 301-306 (2011).
  11. Harraz H.Z. and El-Sharkaway M.F. Origin of tourmaline in the metamorphosed Sikait pelitic belt, South eastern desert, Egypt, *J. Afric. Earth Sci.*, **33**:391-416 (2001).
  12. Hawthorne F.C. and Henry D.J. Classification of the minerals of the tourmaline group. *Eur. J. Mineral.*, **11**: 201-215 (1999).
  13. Hazarika P., Mishra B. and Pruseth K. L. Diverse Tourmaline Compositions from Orogenic Gold Deposits in the Hutt-Maski Greenstone Belt, India: Implications for Sources of Ore-22. Forming Fluids. *Econom. Geol.*, **110**: 337-353 (2015).
  14. Henry D. J. and Dutrow B. L. Evolution of tourmaline in metapelitic rocks: diagenesis to melting, *Geol. Soc. Am. Abstr. Progr.*, **22**:A125 (1990).
  15. Henry D. J. and Dutrow B. L. Metamorphic tourmaline and its petrologic applications. *Rev. Mineral. Geochem.*, **33**, p. (1996).
  16. Henry D.J., Dutrow B.L. and Selvestone J. Compositional asymmetry in replacement tourmaline: an example from the Tauern Window, Eastern Alps. *Geol. Material. Res.*, **4**:1-18 (2002).
  17. Henry D. J. and Guidotti C.V. Tourmaline as petrogenetic indicator mineral: an example from the staurolite-grade metapelites of NW-Maine. *Am. Mineral.*, **70**:1-15 (1985).
  18. Holtz F. and Johannes W. Effect of tourmaline on melt fraction and composition of first melts in quartzofeldspathic gneiss. *Eur. J. Mineral.*, **3**:527-536 (1991).
  19. Kawakami T. Tourmaline and boron as indicators of the presence, segregation and extraction of melt in pelitic migmatites: examples from the Ryoke metamorphic belt, SW Japan. *Transact. Royal Soc. Edinburgh: Earth Sci.*, **95**:111-123 (2004).
  20. Kretz R. Symbols for rock forming minerals. *Am. Mineral.*, **68**:277-279 (1983).
  21. Krosse S. Hochdrucksynthese, Stabilität und Eigenschaften der Borsilikate Dravit und Kornerupin, sowie Darstellung und Stabilitätsverhältnis eines neuen Mg-Al borates. Thesis, Ruhr-Universität Bochum, Germany (1995).
  22. Kutzschbach M., Wunder B., Rhede D., Koch-Müller M., Ertl A., Giester G., Heinrich H. and Franz G. Special Collection: Advances in Ultrahigh-Pressure Metamorphism: Tetrahedral boron in natural and synthetic HP/UHP tourmaline: Evidence from Raman spectroscopy, EMPA, and single-crystal XRD. *Am. Mineral.* **101**:93-104 (2016).
  23. Leeman W. P. and Sisson V. B. Geochemistry of boron and its implications for crustal and mantle processes. Boron: Mineralogy, Petrology and Geochemistry (Grew, E. S. and Anovitz, L. M., eds.), *Min. Soc. Am. Rev. Mineral.*, **33**:645-708 (1996).
  24. London D. Magmatic-hydrothermal transition in the Tanco rare-element pegmatite: Evidence from fluid inclusion and phase equilibrium experiments. *Am. Mineral.*, **71**:376-395 (1986).
  25. London D., Morgan G.B. and Wolf M. B. Boron in granitic rocks and their contact aureoles. In *Mineral. Soc. Am. Rev. Mineral.*, **33**:299-330 (1996).
  26. London D. and Manning D. A. C. Chemical variation and significance of tourmaline from southwest England. *Econom. Geol.*, **90**:495-519 (1995).
  27. Manning D. A. C. Chemical and morphological Variation in tourmalines from the Hub Kapong batholith of Peninsular Thailand. *Min. Mag.*, **45**:139-147 (1982).
  28. Michaeli R. Study of metamorphic rocks from the Gasht and Asalam areas, north Iran. Unpublished Ph.D. thesis. University of Tabriz (2013).
  29. Omrani H., Moazzen M., Oberhänsli R., Tsujimori T., Bousquet R. and Moayyed M. Metamorphic history of glaucophane-paragonite-zoisite eclogites from the Shanderman area, northern Iran. *J. Metamorph. Geol.*, **31**:791-812 (2013a).
  30. Omrani H., Michaeli R. and Moazzen M. Geochemistry and petrogenesis of the Gasht peraluminous granite, western Alborz mountains, Iran. *Neues Jahrb. Geolog. Palaontol. Abhandl.*, **268**:175-189 (2013b).
  31. Ota T., Kobayashi K., Katsura T. and Nakamura E. Tourmaline breakdown in a pelitic system: implications for boron cycling through subduction zones. *Contrib. Mineral. Petrol.*, **155**:19-32 (2008).
  32. Palmer M.R. and Swihart G.H. Boron isotope geochemistry: an overview. In *Boron: Mineralogy, Petrology and Geochemistry* (E.S. Grew & L.M. Anovitz, eds). *Rev. Mineral.* **33**:709-744 (1996).
  33. Robbins C.R. and Yoder H. S. Jr. Stability relations of dravite, a tourmaline. *Carnegie Inst. Wash. Yearbook*, **61**:106-108 (1962).
  34. Spicer E.M., Stevens G. and Buick I.S. The low-pressure partial-melting behaviour of natural boron-bearing metapelites from the Mt. Stafford area, central Australia. *Contrib. Mineral. Petrol.*, **148**:160-170 (2004).
  35. Trumbull R.B. and Chaussidon M. Chemical and boron isotopic composition of magmatic and hydrothermal tourmalines from the Sinceni granite-pegmatite system in Swaziland. *Chem. Geol.*, **153**:125-137 (1999).
  36. Tsang T. and Ghose S. Nuclear magnetic resonance of <sup>1</sup>H,

- $^7\text{Li}$ ,  $^{11}\text{B}$ ,  $^{23}\text{Na}$  and  $^{27}\text{Al}$  in tourmaline (elbaite). *Am. Mineral.*, **58**:224-229 (1973).
37. Ugiyama K. S., Rima H. A., Onno H. K. and Awamata T. K. Distribution of Mn in pink elbaite tourmaline from Mogok, Myanmar. *J. Mineral. Petrol. Sci.* **111**: 1-8 (2016).
38. Van Hinsberg V. J., Henry D. J. and Marschall H. R. Tourmaline: An ideal indicator of its host environment. *Canad. Mineral.*, **49**:1-16 (2011).
39. von Goerne G., Franz G. and Wirth R. Hydrothermal synthesis of large dravite crystals by the chamber method. *Europ. J. Mineral.*, **11**:1061-1078 (1999).
40. Werding G. and Schreyer W. Experimental studies on borosilicates and selected borates. In: Grew E.S. and Anovitz L. M. (EDS) Boron: mineralogy, petrology and geochemistry. *Mineral. Soc. Am.* 2<sup>nd</sup> Ed., **133**:117-163 (2002).
41. Wunder B., Berryman E., Plessen B., Rhede D., Koch-Muller M. and Heinrich W. Synthetic and natural ammonium-bearing tourmaline. *Am. Mineral.*, **100**(1): 250-256 (2015).